JOURNAL OF MATERIALS SCIENCE 23 (1988) 2871–2876

Experimental determination of dynamic Young's modulus and mechanical damping, and theoretical prediction of dislocation density for depleted uranium–0.75 wt % titanium using the PUCOT

K. H. KEENE
Bell Helicopter Textron Inc., Field Investigations Laboratory, PO Box 482, Forth Worth, Texas 76101, USA

A. WOLFENDEN
Mechanical Engineering Department, Texas A&M University, College Station, Texas 77843, USA

G. M. LUDTKA
Development Division, Oak Ridge Y-12 Plant, Oak Ridge, Tennessee 37831, USA

Dynamic Young's modulus (E) and mechanical damping (Q^{-1}) measurements were made for three microstructures (γ, $\alpha + \delta$, and α') of a depleted uranium–0.75 wt % titanium alloy. The temperature range covered was 298 to 1123 K. The apparatus was the piezoelectric ultrasonic composite oscillator technique (PUCOT) operated at 80 kHz. The ranges of values for E and Q^{-1} were 193 to 99 GPa and 3×10^{-3} to 8×10^{-2}, respectively. Correlations for E of each heat treatment as functions of temperature are presented. In addition, the mechanical damping against strain amplitude plots generated from PUCOT data were analysed using the Granato–Luecke zero Kelvin and high-temperature theories of dislocation damping. Computed dislocation densities ranged up to $10^{16}\,m^{-2}$.

1. Introduction

In the science and engineering of materials, knowledge of elastic constants and vibrational damping characteristics are of wide-ranging importance. For example, Young's modulus (E) is used in studies of elasticity, fracture mechanics, creep, thermoelasticity, interatomic forces, etc., as well as for mechanical design purposes. Mechanical damping or internal friction (Q^{-1}) is of critical importance in designs of rotating machinery and in stability of structures of all kinds. On the fundamental side, mechanical damping arises from defects in crystalline materials and its measurement gives us a means of studying defects. This paper gives an account of the determination of dynamic Young's modulus and mechanical damping with the piezoelectric ultrasonic composite oscillator technique (PUCOT) and of the use of the damping data in computing dislocation densities in uranium–0.75 wt % titanium alloys of three heat treatments.

2. Materials tested

The alloy used in this study was fabricated by vacuum-induction melting derby uranium with the titanium sponge in an yttria-coated graphite crucible. The 18 kg, 31 mm thick bookmould casting 127 mm × 178 mm was obtained from the melt by pouring into an yttria-coated graphite mould. This coating reduces the carbon pick-up that can occur in the liquid state to prevent the formation of uranium carbide inclusions that are detrimental to mechanical properties. The composition of the final ingot was (wt %): U 98.75, Ti 0.75, C < 25 p.p.m.

Subsequently, the casting was hot rolled at approximately 590° C from the 31 mm thickness to the final 5 mm thick plate that was supplied as machining stock for the ultrasonic test specimens. The material was rolled down to this thin dimension to facilitate rapid quenching of the plate to ensure development of a fully martensitic microstructure in subsequent heat treatments. A salt bath was used to heat the billet for this rolling procedure. Any hydrogen that may have been picked up by the rolling stock would have outgassed during the subsequent heat treatments in vacuum.

Two separate heat-treatment conditions were studied in this investigation. The first condition involved a solution heat treatment at 800° C for 2 h in vacuum followed immediately by a rapid submersion water quench. The microstructure of this condition is α' martensite. α' is stable only to about 325° C, where it begins to decompose to $\alpha + \delta$ (increasing in rate with increasing temperature). This occurs up to 667° C, at

0022–2461/88 $03.00 + .12

which point the transformation to $\beta + \delta$ takes place. Final transition to γ microstructure is at 723° C.

The second heat treatment initially involved the same solution heat treatment and quenching employed for the first condition. This was followed by an over-ageing heat treatment at 600° C for 5 h. The resultant microstructure is composed of the $\alpha + \delta$ phases with the δ phase present as a fine spheroidal dispersion. The $\alpha + \delta$ microstructure is stable up to 667° C. It becomes $\beta + \delta$ up to 723° C, where transformation to γ phase takes place.

Measurements of the elastic properties for the γ microstructure were made on the α' specimens above the transformation temperature where both microstructures would revert back to γ in this elevated temperature regime. Above about 400° C, the microstructure of the two heat treatments becomes essentially the same; thus testing of both becomes unnecessary. Although uranium alloys have been found to be anisotropic [1], textures of the specimens tested were not known and were thus assumed to be random.

3. Experimental procedure

The piezoelectric ultrasonic composite oscillator technique is a nondestructive method for measuring dynamic Young's modulus, mechanical damping or internal friction and strain amplitude for small specimens. The PUCOT in its present form was first proposed by Robinson and Edgar [2] in 1974. They derived and assessed equations to determine damping, strain amplitude, and Young's modulus from experimentally measured parameters. The PUCOT uses two identical α-quartz piezoelectric crystals (a drive and gauge), a fused quartz spacer rod for temperatures above room temperature and the specimen to be tested. The piezoelectric crystals induce longitudinal, ultrasonic, resonant stress waves in the specimen. For room-temperature measurements, the three-component system is used (Fig. 1). For measurements above room temperature, the four-component system is needed. The fused quartz spacer rod tuned for resonance at the particular test temperature is glued between the piezoelectric crystals and the specimen to keep the piezoelectric crystals at room temperature while the specimen is at high temperature. A closed-loop crystal oscillator is used to drive the system at resonance. A pre-selected gauge voltage is maintained by the oscillator to obtain a constant strain amplitude. The values of the drive crystal voltage, gauge crystal voltage, period of the three- or four-component system, and specimen temperature are measured. These measured values can be used to calculate dynamic Young's modulus, mechanical damping and strain amplitude using standard equations [2–4].

As the specimens tested are radioactive, precautions were observed to minimize exposure to radiation. The main health hazard from depleted uranium is its heavy metal toxicity [5]. A vacuum system with a gas washing filter was constructed to prevent the inhalation of any dust or oxides produced. In addition, all the required cutting and grinding of the specimens were performed in a glove box. More details have been given elsewhere [6]. The vacuum and gas washing filter systems and the PUCOT are shown schematically in Fig. 2.

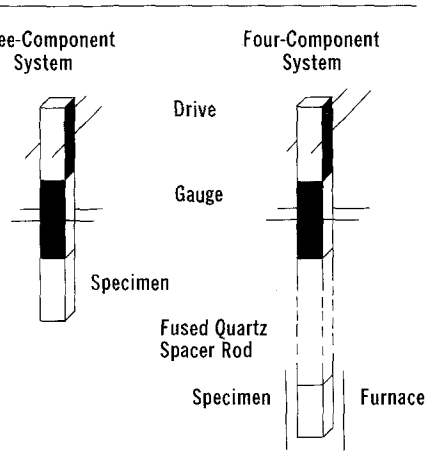

Figure 1 Schematic diagram of the essential components of the piezoelectric ultrasonic composite oscillator technique (PUCOT).

4. Granato–Luecke zero Kelvin analysis

A theory of dislocation damping, first proposed in 1956 by Granato and Luecke [7, 8], relates damping and modulus effects to dislocations in materials. This theory is based on Koehler's [9] model which consists of a pinned dislocation loop oscillating due to an applied alternating stress. The model is analogous to a string under forced damped vibration and is thus known as the vibrating string model. The theory allows for two types of damping (Fig. 3): the first type is strain amplitude independent (Q_I^{-1}) and occurs at frequencies in the kilohertz range; the second type is strain amplitude dependent (Q_H^{-1}) and is a maximum in the high megahertz range.

This theory assumes that a dislocation double loop exists with minor pinning lengths, l_1 and l_2, whose lengths are much less than the network length (L_N). The stress which is imposed on the dislocation pinning point increases as the sum of the lengths of the adjacent minor pinning point lengths increases. Dislocation break-away must occur at the dislocation double loop pinning point where the sum of adjacent minor pinning lengths is greatest. A chain reaction involving dislocation break-away of the entire network length results. The Granato–Luecke zero Kelvin (GLOK) plot is constructed by plotting the strain amplitude times the strain amplitude dependent damping against the inverse of the strain amplitude. An example of a GLOK plot for α' specimens at 100° C is shown in Fig. 4. The slope of the GLOK plot must be negative in order to perform the analysis.

The assumptions made in the original Granato–Luecke papers [7, 8] are:

1. The theory is formulated for 0 K, i.e. where the thermal activation is zero.
2. Dislocation break-away is purely mechanical in origin.
3. Dislocations may be pinned by impurities such as impurity atoms, vacancies, and second-phase particles.
4. Pinning point lengths are assumed to be random in nature.

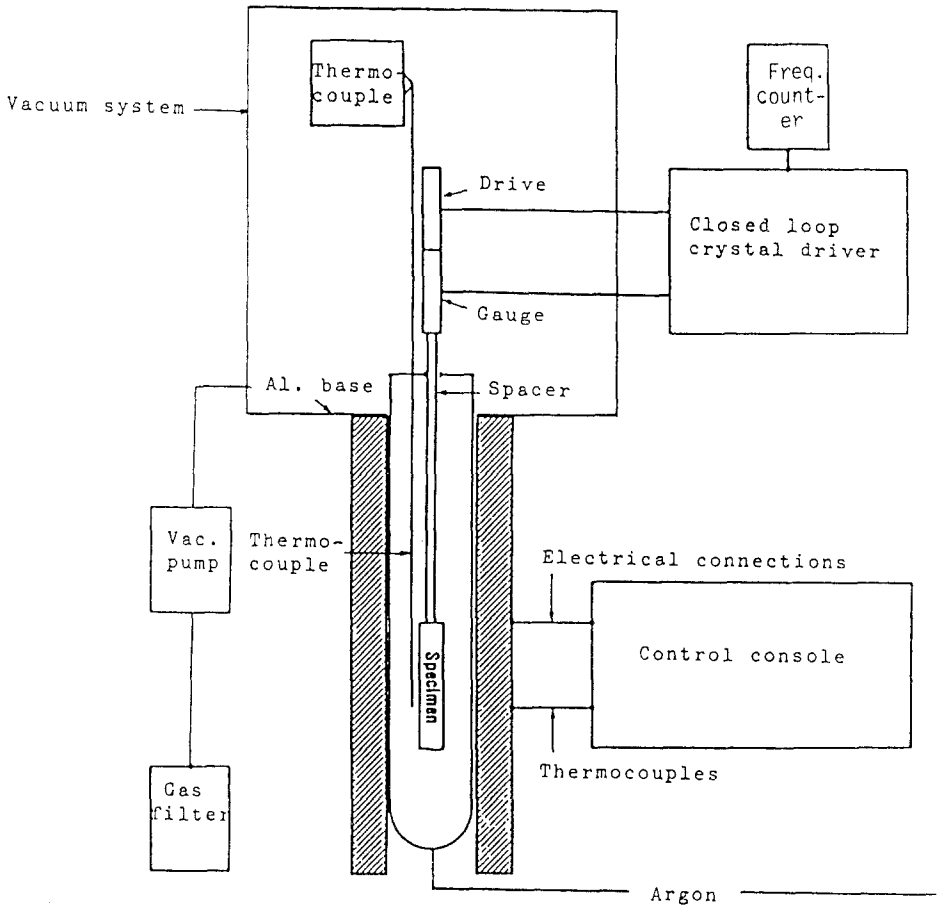

Figure 2 Schematic diagram of the entire apparatus for determining modulus and damping in the uranium alloys. Note the vacuum and gas filter systems.

5. Strain amplitude independent damping is the result of dislocation resonance.
6. Strain amplitude dependent damping is the result of dislocation break-away and is a hysteresis type loss.
7. Dislocation break-away is sequential in nature.

5. Granato–Luecke high-temperature analysis

A second theory of dislocation damping proposed by Granato and Luecke in 1981 [10] allows damping effects at high temperatures to be analysed. Known as the Granato–Luecke high-temperature (GLHT) theory of dislocation damping, this theory includes consideration of the thermal activation energy. This, in turn, allows for the thermal vibration within the lattice to contribute to dislocation break-away. Here, dislocation break-away is assumed to be primarily thermal in origin.

The effective activation energy is known to vary with the number of dislocation pinning points, and inversely with the stress required to initiate dislocation break-away. Dislocation break-away must now occur at multiple pinning points simultaneously because the mechanism for dislocation double loop break-away no longer exists. In other words, the energy of the dislocation break-away state of a double loop dislocation is higher than that of the pinned dislocation state. Dislocation break-away can now occur at stresses much lower than those in the GLOK theory. The GLHT plot is constructed by plotting the strain amplitude dependent damping divided by the strain amplitude against the inverse of the strain amplitude. The slope of the GLHT plot must be negative in order to perform the analysis.

The assumptions made in the GLHT theory of dislocation damping are:

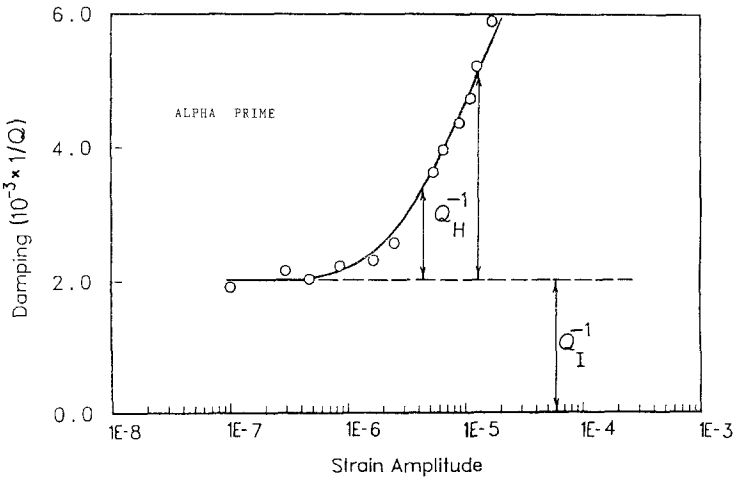

Figure 3 Strain amplitude independent (Q_I^{-1}) and strain amplitude dependent (Q_H^{-1}) damping in U–0.75 wt % Ti.

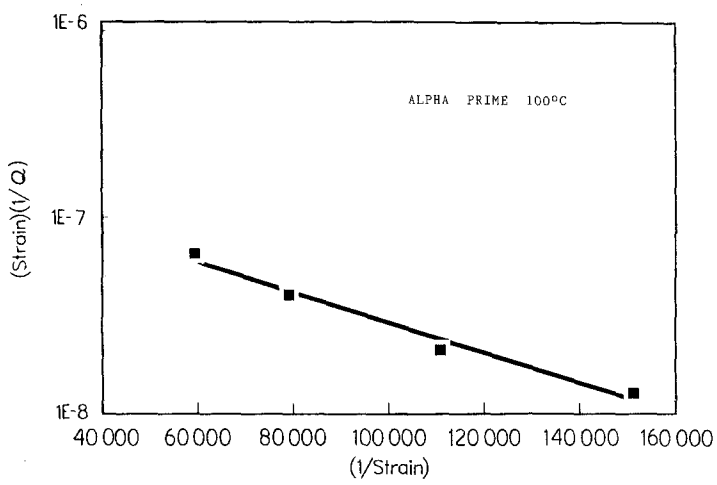

Figure 4 A Granato–Luecke 0 K plot for α' U–0.75 wt % Ti at 100° C.

1. The theory applies to temperatures greater than 0 K.
2. Dislocation break-away is primarily thermal in origin.
3. Dislocations may be pinned by impurities such as impurity atoms, vacancies, and second-phase particles.
4. Pinning point lengths are assumed to be random in nature.
5. Strain amplitude independent damping is the result of dislocation resonance.
6. Strain amplitude dependent damping is the result of dislocation break-away and is a hysteresis type loss.
7. Dislocation break-away is simultaneous in nature.

6. Results and discussion

6.1. Young's modulus

Dynamic Young's modulus results for the three microstructures α', $\alpha + \delta$ and γ are shown graphically in Fig. 5. Table I gives the best fit equation, the determination coefficient (R^2) and the standard error of estimate (SE) for each microstructure.

First-order curves were selected for the Young's modulus data for the $\alpha + \delta$ and γ specimens, while a second-order curve fit was selected for the α' specimens. Values of R^2 ranged from 0.960 for the $\alpha + \delta$ specimens to 0.988 for the gamma specimens. The standard error of estimate ranged from 4.7 GPa for the $\alpha + \delta$ specimens to 0.06 GPa for the γ specimens. A slight anomaly in the Young's modulus data of the $\alpha + \delta$ specimens was observed at a temperature of about 475° C. The greatest amount of data scatter is obvious in the region of 400 to 500° C as can be seen when this region is compared to other portions of Fig. 5. This data scatter for the $\alpha + \delta$ specimens resulted in the lowest determination coefficient.

It was noted above that a second-order curve fit was selected for the Young's modulus data obtained for the α' specimens. This levelling off trend near 400° C in Young's modulus with increasing temperature may be the result of the precipitation of second-phase particles. Further details of Young's modulus, shear modulus and Poisson's ratio for these specimens have been presented earlier [6].

Finally, in this section on the temperature dependence of Young's modulus, we shall apply what we term a Friedel analysis [11] to the E against T relations. Friedel made a tabulation of the term $-(1/E)(dE/dT)$ for several metals and found that the term fell in the range 4 to 14 $\times$ $10^{-4}K^{-1}$. From the relations given in Table I, and with the term dE/dT being obtained as the differential of $E = E(T)$, the values of $-(1/E)(dE/dT)$ for the various microstructures lie in the range 2.8 $\times$ 10^{-4} to 7.1 $\times$ $10^{-4}K^{-1}$ for α' U–Ti and 3.6 $\times$ 10^{-4} to 4.6 $\times$ $10^{-4}K^{-1}$ for $\alpha' + \delta$ U–Ti. However, for the γ U–Ti, the term lies near 5 $\times$ $10^{-5}K^{-1}$. Clearly then, the α' U–Ti and the $\alpha' + \delta$ U–Ti yield values of $-(1/E)(dE/dT)$ which conform to those listed by Friedel, whereas the γ U–Ti has values outside this range.

6.2. Mechanical damping

Mechanical damping, or internal friction (Q^{-1}), against strain amplitude curves plotted from PUCOT

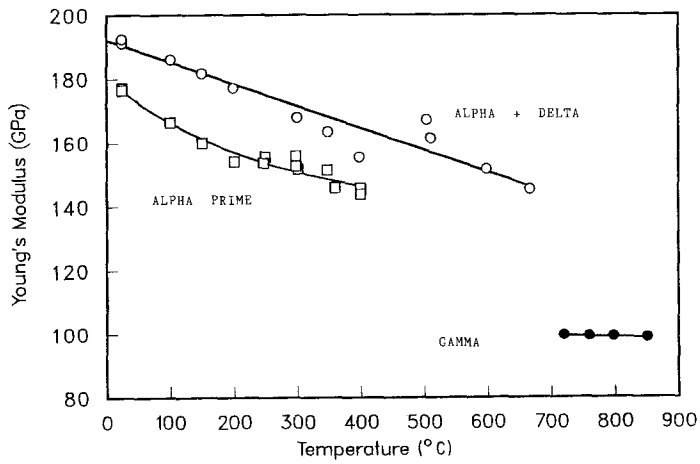

Figure 5 Dynamic Young's modulus as a function of temperature for U–0.75 wt % Ti in three conditions of heat treatment.

TABLE I Dynamic Young's modulus equations for U–0.75 wt % Ti

α'	$E = 179.403 - 0.130\,(T) + 0.000\,117\,(T^2)$ GPa	
	$SE = 2.21$ GPa $\quad R^2 = 0.986$	(T in °C)
$\alpha + \delta$	$E = 191.974 - 0.0682\,(T)$ GPa	
	$SE = 4.70$ GPa $\quad R^2 = 0.960$	
γ	$E = 103.347 - 0.00511\,(T)$ GPa	
	$SE = 0.06$ GPa $\quad R^2 = 0.988$	

data for specimens at 23, 100 and 200° C are shown in Fig. 6. These plots exhibit the typical strain amplitude independent (Q_I^{-1}) and strain amplitude dependent (Q_H^{-1}) behaviour of most crystalline materials.

The α' specimens exhibited higher damping than did the $\alpha + \delta$ specimens as can be seen from Fig. 6. The strain independent damping values ranged from 2×10^{-3} to 8×10^{-2} for the α' specimens and from 3×10^{-4} to 3×10^{-2} for the $\alpha + \delta$ specimens. The mechanical damping against strain amplitude plots were used to calculate dislocation density and minor pinning lengths for the specimens in the Granato–Luecke analysis sections of this paper.

It is interesting to compare the levels of mechanical damping measured in the U–Ti specimens to levels of damping observed for another heavy metal, namely, lead. For strain amplitudes in the range 10^{-6} to 10^{-3}, Mason [12] has documented damping levels of 5×10^{-4} to 3×10^{-2} in 99.99% pure lead, and for lead of various purities, and at stress levels in the range 0.07 to 7 MPa, damping levels of 2×10^{-2} to 2×10^{-1}. Our range of values of Q^{-1} was 3×10^{-3} to 8×10^{-2} for the U–Ti alloys with stresses in the range 0.02 to 20 MPa. Thus, there is quite an overlap of the damping values for the two different heavy materials.

6.3. Granato–Luecke 0 K results

GLOK analysis of the α' specimens yielded minor pinning lengths on the order of 10^{-8} m, and mobile dislocation densities on the order of 10^{13} to 10^{16} m^{-2}. GLOK analysis of the $\alpha + \delta$ specimens yielded minor pinning lengths on the order of 10^{-8} to 10^{-9} m, and mobile dislocation densities on the order of 10^{12} to 10^{15} m^{-2}. Minor pinning lengths and mobile dislocation densities calculated using the GLOK theory are given in Table II. These values are typical of experimentally determined dislocation densities in other metals (Table III) and await confirmation by electron microscopy. The calculated minor pinning lengths are of reasonable magnitude. These calculations indicate that the GLOK theory gives reasonable predictions for these specimens at temperatures higher than those envisaged by Granato and Luecke.

TABLE II GLOK theory results

Specimen	Temperature (° C)	Network length (m)	Minor pinning length (m)	Dislocation density (m^{-2})
$\alpha + \delta$	100	1×10^{-5}	2×10^{-9}	4×10^{12}
	100	1×10^{-6}	2×10^{-9}	4×10^{15}
	500	1×10^{-5}	3×10^{-8}	7×10^{12}
	500	1×10^{-6}	3×10^{-8}	7×10^{15}
α'	24	1×10^{-5}	3×10^{-8}	2×10^{13}
	24	1×10^{-6}	3×10^{-8}	2×10^{16}
	100	1×10^{-5}	6×10^{-8}	7×10^{13}
	100	1×10^{-6}	6×10^{-8}	7×10^{16}
	200	1×10^{-5}	7×10^{-8}	2×10^{13}
	200	1×10^{-6}	7×10^{-8}	2×10^{16}

6.4. Granato–Luecke high-temperature results

GLHT analysis of the α' specimens yielded minor pinning lengths on the order of 10^{-9} m, and mobile dislocation densities on the order of 10^{6} m^{-2}. GLHT analysis of the $\alpha + \delta$ specimens yielded minor pinning lengths on the order of 10^{-8} to 10^{-9} m, and mobile dislocation densities on the order of 10^{6} to 10^{7} m^{-2}. Minor pinning lengths and mobile dislocation densities calculated using the GLHT theory are given in Table IV.

The values predicted for the minor pinning length by the GLHT theory are of the same order of magnitude as expected minor pinning lengths in other metals. However, the mobile dislocation densities predicted by this theory are several orders of magnitude lower than experimentally determined results for other metals. Therefore, the GLHT theory does not yield reasonable values for the mobile dislocation density for these materials. A similar conclusion was reached by Hartman *et al.* [14] who studied dislocation damping effects in several metal matrix composites. The inability of this theory to determine reasonable mobile dislocation densities may be due to the fact that the exact relationship for the interaction between dislocations and pinning points at high temperatures

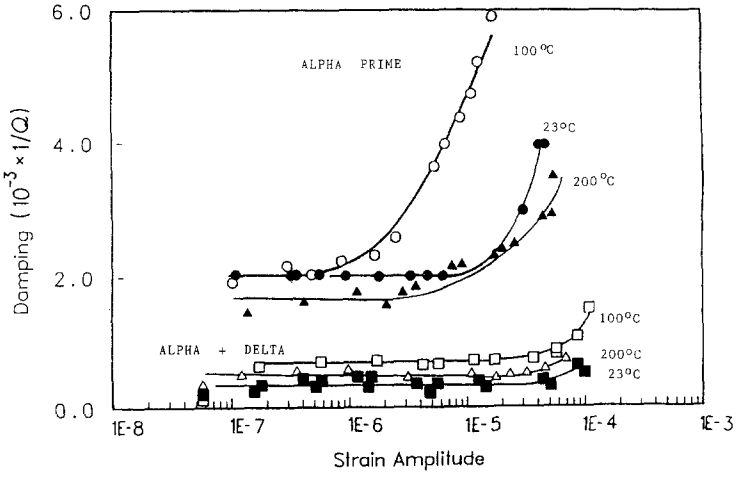

Figure 6 Amplitude dependence of damping in α' and $\alpha + \delta$ U–0.75 wt % Ti for several temperatures.

TABLE III Typical dislocation densities

Material	Reference	Dislocation density (m^{-2})
Silver	[13]	$2 \times 10^{14} - 7 \times 10^{14}$
Copper	[13]	1×10^{14}
Iron	[11]	1×10^{15}
Tin	[11]	1×10^{13}
Aluminium	[11, 12]	$1 \times 10^{14} - 2 \times 10^{14}$
"Typical"	[11]	$1 \times 10^{10} - 1 \times 10^{16}$

is not known. Electron microscopy observations are expected to be helpful in explaining why the GLHT theory does not work for these materials.

7. Conclusions

This investigation of the dynamic Young's modulus and mechanical damping for U–0.75 wt % Ti alloys with three microstructures leads to the following conclusions.

1. Dynamic Young's modulus (E) for the three microstructures can be obtained from the equations given in Table I.

2. The normalized temperature dependence of Young's modulus $[-(1/E)(dE/dT)]$ for α' U–Ti was found to be in the range 3 to 7 $\times$ $10^{-4}K^{-1}$ and that for $\alpha' + \delta$ near 4 $\times$ $10^{-4}K^{-1}$, while the dependence for γ U–Ti was about 5 $\times$ $10^{-5}K^{-1}$. These values compare with the range documented by Friedel for several metals of 4 to 14 $\times$ $10^{-4}K^{-1}$.

3. The α' specimens exhibited higher damping than did the $\alpha + \delta$ specimens. The strain amplitude independent damping values ranged from 2 $\times$ 10^{-3} to 8 $\times$ 10^{-2} for the α' specimens and from 3 $\times$ 10^{-4} to 3 $\times$ 10^{-2} for the $\alpha + \delta$ specimens.

4. The Granato–Luecke 0 K theory yielded mobile dislocation densities for the α' specimens that ranged from 10^{13} to $10^{16}m^{-2}$ and minor pinning lengths on the order of 10^{-8} m.

5. The Granato–Luecke 0 K theory yielded mobile dislocation densities for the $\alpha + \delta$ specimens that ranged from 10^{12} to $10^{15}m^{-2}$ and minor pinning lengths on the order of 10^{-9} to 10^{-8} m.

6. The Granato–Luecke high temperature theory yielded mobile dislocation densities for the α' specimens on the order of $10^{6}m^{-2}$ and minor pinning lengths on the order of 10^{-8} m.

7. The Granato-Luecke high-temperature theory yielded mobile dislocation densities for the $\alpha + \delta$ specimens that ranged from 10^{6} to $10^{7}m^{-2}$ and minor pinning lengths on the order of 10^{-8} m.

8. The Granato–Luecke 0 K theory yielded more realistic values for the mobile dislocation density for these materials than did the Granato–Luecke high-temperature theory.

TABLE IV GLHT theory results

Specimen	Temperature (°C)	Network length (m)	Minor pinning (m)	Dislocation density (m^{-2})
$\alpha + \delta$	100	1×10^{-6}	2×10^{-8}	3×10^{7}
	100	1×10^{-7}	9×10^{-8}	1×10^{7}
	500	1×10^{-7}	7×10^{-8}	2×10^{6}
α'	24	Slope of GLHT plot positive, no test		
	100	Slope of GLHT plot positive, no test		
	200	1×10^{-7}	4×10^{-8}	4×10^{6}

Acknowledgement

This research was sponsored by Martin Marietta Energy Systems Inc., Oak Ridge Y-12 Plant, under contract no. DE-AC05-840R21400 for the US Department of Energy.

References

1. Roy A. VANDERMEER, Proceedings Metallurgical Technology of Uranium and Uranium Alloys, 26–28 May (American Society for Metals, Metals Park, Ohio, 1982).
2. W. H. ROBINSON and A. EDGAR, *Trans. Sonics Ultrasonics* **SU-21** (2) (1974) 98.
3. A. WOLFENDEN and W. H. ROBINSON, Proceedings of 1975 Metals Congress, Australian Institute of Metals, Adelaide, South Australia, 12–16 May (1975).
4. *Idem, Scripta Metall.* **10** (1976) 763.
5. P. LOWENSTEIN, "Metals Handbook", Vol. 3, 9th Edn (American Society for Metals, Metals Park, Ohio, 1980) pp. 773–80.
6. K. H. KEENE, J. T. HARTMAN Jr, A. WOLFENDEN and G. M. LUDTKA, *J. Nucl. Mater.* **149** (1987) 218.
7. A. GRANATO and K. LUECKE, *J. Appl. Phys.* **27** (1956) 583.
8. *Idem, ibid.* **27** (1956) 789.
9. J. S. KOEHLER, "Imperfections in Nearly Perfect Crystals" (Wiley, New York, 1952) p. 197.
10. A. GRANATO and K. LUECKE, *J. Appl. Phys.* **52** (1981) 7136.
11. Jacques FRIEDEL, "Dislocations" (Addison Wesley, Reading, Massachusetts, 1964) pp. 211, 273, 407, 411 and 413; and Appendix B, 454–457.
12. W. P. MASON, "Internal Friction, Plastic Strain and Fatigue in Metals and Semiconductors", ASTM STP no. 237 (American Society for Testing and Materials, Philadelphia, Pennsylvannia, 1958) p. 36.
13. M. B. BEVER, D. L. HOLT and A. L. TITCHENER, "The Stored Energy of Cold Work" (Pergamon, Oxford, 1973) pp. 133, 147.
14. J. T. HARTMAN Jr, K. H. KEENE, R. J. ARMSTRONG and A. WOLFENDEN, *J. Metals* (April) (1986) 33.

Received 23 August
and accepted 1 December 1987